Gust Load Alleviation Using Nonlinear Feedforward Control

Maryam Ghandchi Tehrani[1], Andrea Da Ronch[2]
[1]Institute of Sound and Vibration Research, Faculty of Engineering and Environment
University of Southampton, Southampton, SO17 1BJ, UK
[2]Faculty of Engineering and Environment, University of Southampton, Southampton, SO17 1BJ, UK
Email: m.ghandchi-tehrani@soton.ac.uk, a.da-ronch@soton.ac.uk

ABSTRACT: A strategy based on feedforward control for gust loads alleviation of a nonlinear aeroelastic model is considered. The model is representative of a typical wing section with a trailing-edge flap and with a polynomial nonlinearity in the structural model. The aerodynamics is given by thin aerofoil theory. First, the effects of structural nonlinearity in the dynamic response of the open-loop system are evaluated. Then, it is shown that the performance of the controller is greatly affected by the approximations made in the internal model of the controlled plant. To suppress gust-induced vibrations of an intrinsically nonlinear plant, the control performance is degraded when using a linear representation for the internal model. The control strategy performs well when including all nonlinearities in the model.

KEY WORDS: Feedforward control, aeroelastic model, gust response

1 INTRODUCTION

Time-domain analyses of highly flexible aerial vehicles encountering atmospheric turbulence are still expensive despite the increase in today's computing power. The simulation costs become prohibitive when high-fidelity numerical models are introduced in an industrial environment with a very large number of simulations required. Parametric searches are performed to estimate the critical loads that the aircraft will encounter during the expected life cycle and these are used for structural sizing. Inaccuracies in the load estimates can jeopardise the entire project or result in a very conservative (and inefficient) design.

Active control has the potential to increase aircraft performance (by reducing structural weight) and extend the flight envelope. The design of a gust-tolerant vehicle needs an accurate model to realistically simulate the non-linear interactions that dominate such aerial platforms. Nevertheless, the use of fairly large non-linear physics-based models introduces a complication in the design, synthesis, and testing of control strategies.

Traditionally, model reduction techniques are used to generate a system of small size that is less expensive to solve than the original full order model. There are two approaches to model reduction. The first approach is based on system identification, where known inputs and measured outputs are used to create a model of the original system, which is treated as a black-box. These methods lack robustness and are limited by the amount of training data used to generate them, but have been applied successfully, see Ref. [1]. The second approach is based on a manipulation of the equations of the original system to make calculations more efficient. These methods are only limited by the approximations introduced in the model formulation, see Ref. [2].

With the previous paragraphs as background, to make progress in this research work, we explore the use of a nonlinear control strategy to control the gust-induced vibrations of a nonlinear aeroelastic model. The test case is for a typical wing section with structural nonlinearities, with the aerodynamics given by two-dimensional thin aerofoil theory. The future direction of this work is to expand the approach herein described to larger computational models by using the nonlinear model reduction of Ref. [2]. This would open up the possibility of investigating the performance of novel nonlinear control strategies applied to a smaller system that retains the most dominant nonlinear effects of the original full order model.

The feedforward algorithm used herein is well-established in active control and is mainly used for linear systems [3]. In contrast to feedback control, feedforward control requires the knowledge of the disturbance signal; therefore it is more attractive for systems where the frequency of the disturbance signal is known. As one example, in helicopters the disturbance frequency is multiple integer of the blade passing frequency or, in cars, the engine noise frequency can be determined from the engine speed. The control force will be obtained by minimizing the error between the disturbance signal and the secondary force generated by the actuators. To achieve this, an estimate of the physical system, known as internal model, is required. If the internal model does not include the effect of nonlinearities and is only based on the information of the linear system, the performance of the control system is reduced and vibration suppression cannot be achieved.

The paper continues with a formulation of the aeroelastic model used to model the dynamics of a typical wing section. A control strategy based on feedforward control is then described. The performance of the controller is illustrated on the aeroelastic model with and without the structural nonlinearities. Finally, conclusions are given.

2 AEROELASTIC MODEL FORMULATION

The coupled aeroelastic model follows the formulation presented in Ref. [2]. The aerofoil section shown in Fig. 1 has two degrees of freedom that define the motion about a

reference elastic axis (e.a.). The plunge deflection is denoted by h, positive downward, and α is the angle of attack about the elastic axis, positive with nose up. The motion is restrained by two springs, K_ξ and K_α, and is assumed to have a horizontal equilibrium position at $h = \alpha = 0$. Structural damping in both degrees of freedom is also included in the system. A trailing-edge flap, which is assumed massless in this study, is used in combination with an active control system to extend the stable flight region and for gust loads alleviation.

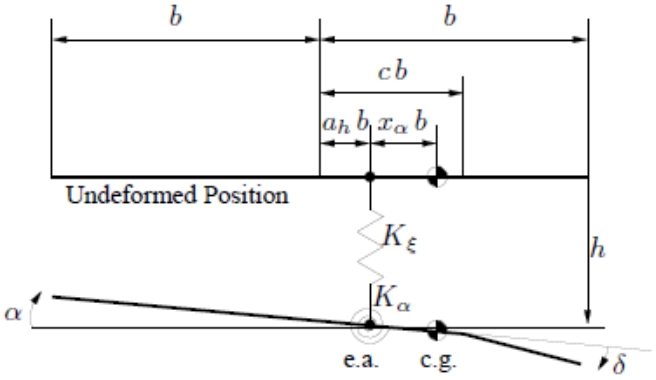

Figure 1. Schematic of the typical wing section; the wind speed is from the right and horizontal

Several options for the aerodynamics can be used. For an irrotational and incompressible two-dimensional flow, the aerodynamic model is given by the classical theory of Theodorsen. The total aerodynamic loads consist of contributions arising from the section motion (pitch and plunge), flap deflection, and the penetration into a gusty field. The aerodynamic loads due to an arbitrary input time-history are obtained through convolution against a kernel function. Since the assumption is of linear aerodynamics, the effects of the various influences on the aerodynamic forces and moments are added together to find the variation of the forces and moments in time for a given motion and gust.

A detailed derivation of the aeroelastic model can be found in Ref. [4]. In this work, the structural nonlinearity in the stiffness terms is modelled using a polynomial form. The resulting coupled aeroelastic model is expressed in the form of a set of nonlinear ordinary differential equations. The system parameters, here not included for brevity, are chosen from Ref. [5].

3 WORST-CASE GUST

The aeroelastic response to a gust vertical disturbance is studied at 95% of the linear flutter speed. At this flight conditions, the pitch and plunge frequencies are close to each other, and will coalesce for increasing speed at the instability point (flutter). For the "one-minus-cosine" gust family, a parametric search was done to find the gust wavelength that causes the largest structural response. The response in the pitch degree of freedom (wing torsion) was taken as figure of merit. Once the gust wavelength that causes the largest pitch response is identified, the gust vertical velocity was increased in the range of 0.005 to 0.1 (normalized by the freestream speed) to evaluate the effect of the structural nonlinearity. Here, the cubic term of the pitch stiffness is chosen to be 3.0 (hardening spring type). The time domain response of the typical wing section was then used to calculate the transfer function for each particular gust vertical velocity.

4 FEEDFORWARD CONTROL

Feedforward control is used to control the vibrations of the pitch and plunge modes. Here single-input-single-output control is considered. The transfer function of the physical system G is obtained from the above aeroelastic calculations and w is the adaptive filter or controller.

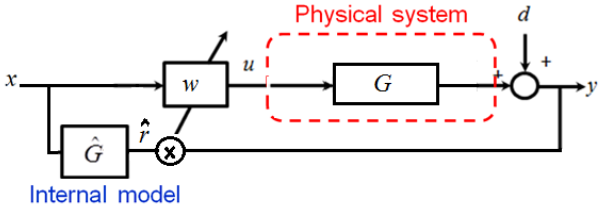

Figure 2. Adaptive feedforward control

In the block diagram in Fig. 2, d is the disturbance signal (gust vertical velocity in the aeroelastic model), x is the reference signal, $\hat{r}$ is the filtered reference signal, and y is the vibration error signal. The objective is to design a control force u to minimize the vibration level y at the location on the wing. This vibration signal can be represented as

$$y(n) = d(n) + Gw(n)x(n) \tag{1}$$

The coefficient of the controller is updated at each iteration n to adjust the amplitude and phase of the reference signal x in order to cancel the disturbance d [6]. This requires an estimate of the internal model $\hat{G}$. The performance of the feedforward algorithm depends on the accuracy of the estimated internal model.

$$w(n+1) = w(n) - \alpha\hat{r}(n)y(n) \tag{2}$$

In Eq. (2), α is the convergence coefficient and for the linear model the maximum convergence rate is $2/(\hat{G}^H\hat{G})$. If the physical system is nonlinear, and the estimate of the internal model is based on the linear model, then the performance of the controller is reduced and the convergence of the algorithm is also affected.

4.1 Linear Plant

The transfer functions of the pitch and plunge motions are plotted in Figs. 2 and 3. A curve fitting technique in Matlab is used to obtain the transfer function of the physical model in the complex *s*-domain. The curve fitted technique is detailed in Ref. [7] for pole placement using feedback control. The curve fitted model is accurate near the pitch and plunge modes, around 1.5 to 2.5Hz.

A Simulink model is built to control the pitch and plunge modes using the block diagram in Fig. 2. The internal model is obtained from the curve fitted model at the frequency of the pitch and plunge modes. A reference signal is generated $x(n) = 0.01\, e^{i\omega_0 n}$, where ω_0 is the frequency of

pitch (2.52 Hz) or plunge (1.74 Hz) mode. The coefficient of the controller is updated to minimize the vibration at that particular frequency. The convergence rate is defined as $\alpha = 5 \cdot 10^{-6}$.

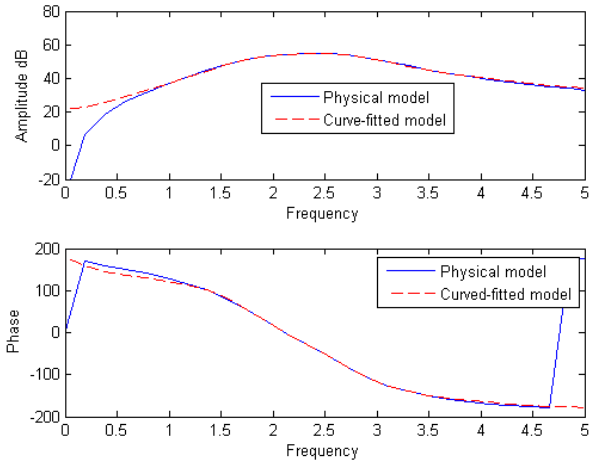

Figure 2. Pitch mode: Receptance: physical model (blue solid line) and curve fitted model (red dashed line)

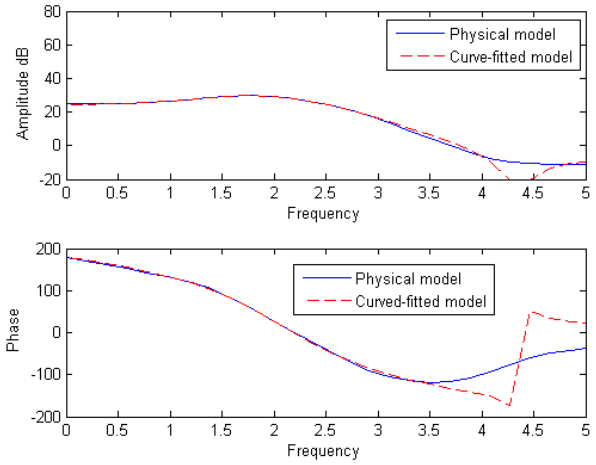

Figure 3. Plunge mode: Receptance: physical model (blue solid line) and curvefitted model (red dashed line)

Pitch control. The disturbance signal and the controlled response are shown in Fig. 4. The internal model is estimated to have the value of $\hat{G}(i\omega_0) = 306 - 442i$ at the pitch frequency. It can be seen that the vibration level is minimized after 60 iterations. The real and imaginary part of the control force u required to cancel the vibrations are shown in Fig. 5. From Fig. 6, the real and imaginary parts of the filter coefficient are converged to $w_R = -1.8 \cdot 10^{-3}$ and $w_I = -1.7 \cdot 10^{-3}$, respectively.

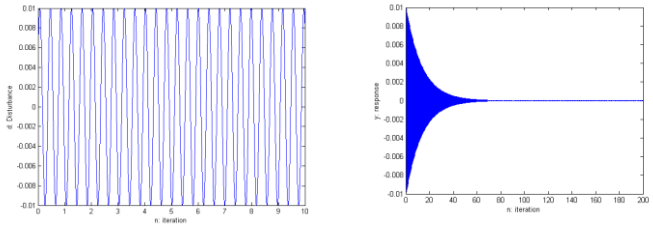

(a) (b)

Figure 4. Pitch control: (a) disturbance d, (b) controlled response y versus iteration

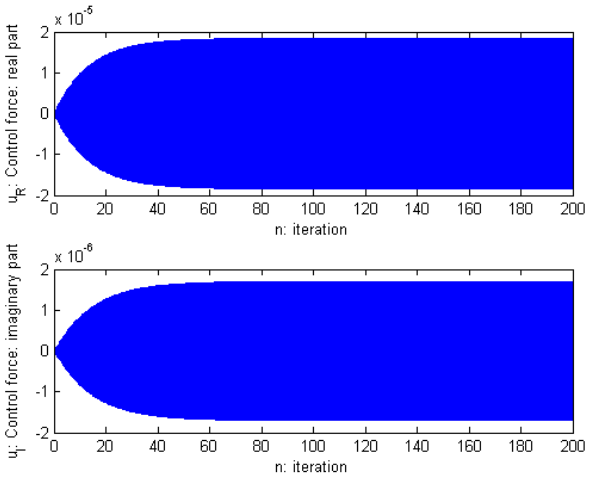

Figure 5. Pitch control: real and imaginary part of the control force $u(n)$

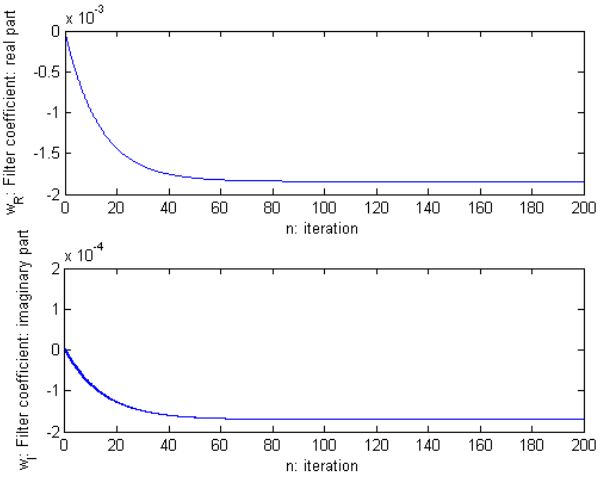

Figure 6. Pitch control: real and imaginary part of the filter coefficient $w(n)$

Plunge control. Simulations were carried out to control the plunge mode at 1.74 Hz. The internal model at that frequency is $\hat{G}(i\omega_0) = 15.11 + 27.3i$, and the convergence rate is chosen equal to $\alpha = 5 \cdot 10^{-3}$.

The disturbance and the controlled plunge response are shown in Fig. 7.

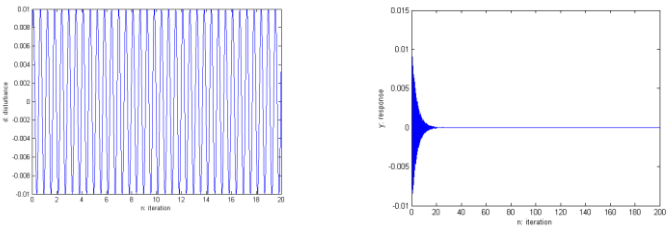

(a) (b)

Figure 7. Plunge control: (a) disturbance d, (b) controlled response y versus iteration

The response is controlled after 20 iteration. This is due to the accurate estimation of the physical model. The control force and the filter coefficient are also shown in Figs. 8 and 9. The coefficients of the filter are converged to $w_I = -1.7 \cdot 2$ and $w_I = -2.8 \cdot 10^{-2}$, respectively.

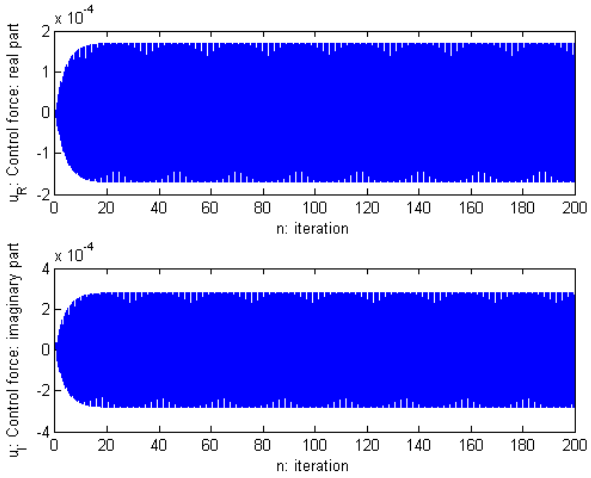

Figure 8. Plunge control: real and imaginary part of the control force $u(n)$

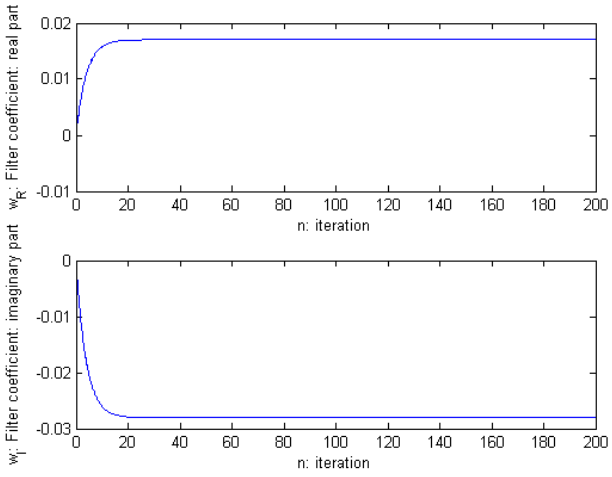

Figure 9. Plunge control: real and imaginary part of the filter coefficient $w(n)$

4.2 *Nonlinear Plant*

In this section, the physical system has nonlinear behavior and the performance of the control algorithm when the internal model is based on the linear model, in which the nonlinearities are neglected, will be compared with the case when the internal model is an accurate representation of the physical nonlinear model.

The transfer functions are obtained for two degrees of freedom with different input amplitudes. By increasing the amplitude of the gust load, the nonlinearities in the response become more evident as shown in Figs. 10 and 11. This clearly demonstrates that nonlinearity has effect on the response and the performance of the control algorithm is affected.

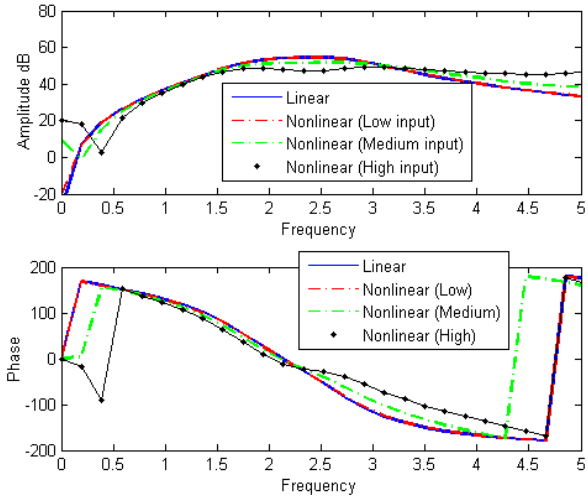

Figure 10. Nonlinear behavior for different input levels: transfer function represents the pitch mode

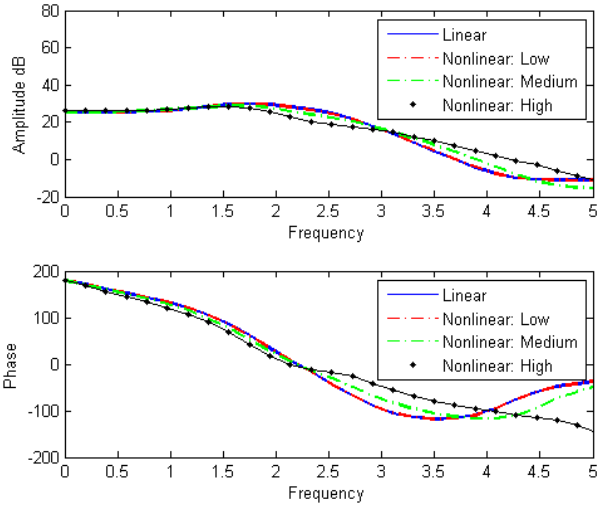

Figure 11. Nonlinear behavior for different input levels: transfer function represents the plunge mode

The receptances are curve fitted to obtain the transfer function in the *s*-domain to represent the physical model. There is a good agreement between the physical and the fitted model in the vicinity of the pitch and plunge modes, as can be seen from Figs. 12 and 13.

Pitch control. Simulations were carried out to control the pitch mode using feedforward control. Two estimates of internal model are considered for comparison.

Case1. The nonlinearity is neglected and $\hat{G}$ is based on the linear model. The value at the pitch frequency is $\hat{G} = 306 - 442i$.

Case2. The nonlinearity is included and $\hat{G}$ is based on the nonlinear model. The value at the pitch frequency is $\hat{G} = 199 - 108i$.

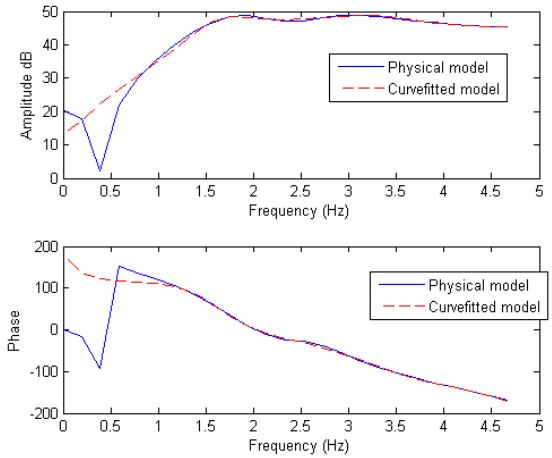

Figure 12. Nonlinear receptance for high input amplitude: physical model (blue solid line) and curve fitted model (red dashed line): location

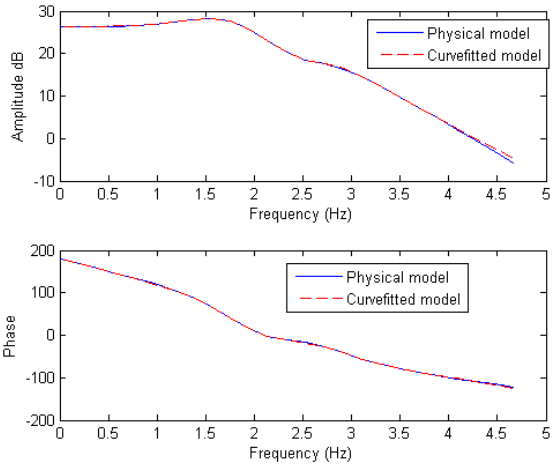

Figure 13. Nonlinear receptance for high input amplitude: physical model (blue solid line) and curve fitted model (red dashed line): location

The results are compared for the two casesin Figs 14 to 16. The blue dashed line represents case 1, when the nonlinearities are ignored in the internal model and the red solid line represents case 2, when the nonlinear model is considered. For case 2, the control algorithm converges faster and the vibration response is minimized with smaller number of iterations as shown in Figs. 14 and 15. The convergence of the controller gains as function of the iterations is shown in Fig. 16 for the linear and nonlinear cases.

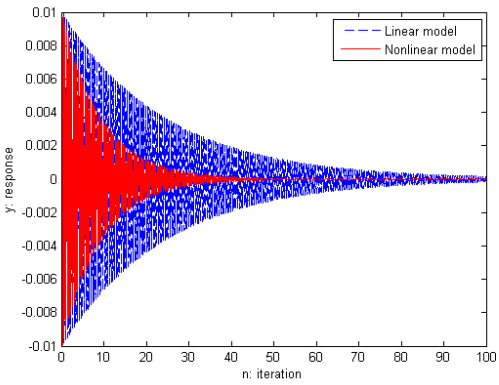

Figure 14. Pitch control: vibration response using linear (blue dashed line) and nonlinear model (red solid line)

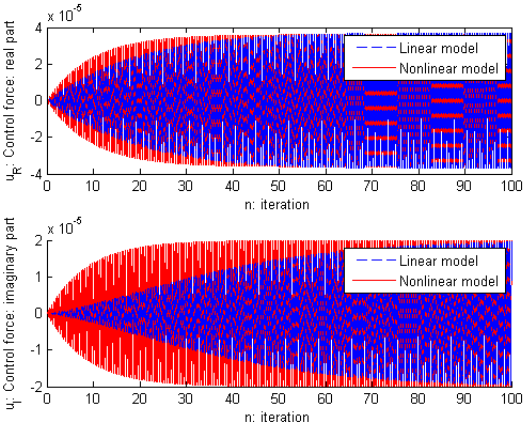

Figure 15. Pitch control force: linear (blue dashed line) and nonlinear model (red solid line)

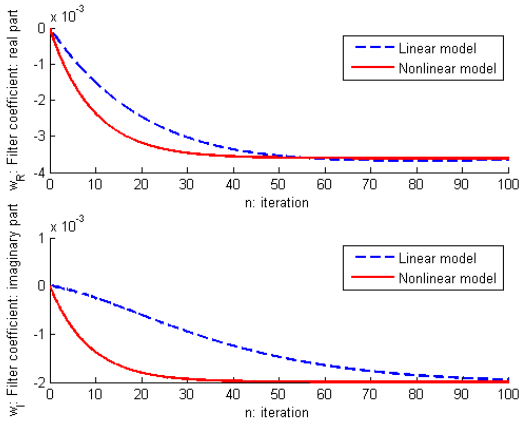

Figure 16. Pitch control: Filter coefficient for the linear (blue dashed line) and nonlinear model (red solid line)

Plunge control. Similarly, we control the plunge mode, considering the two cases.

Case1. Nonlinearity is neglected and $\hat{G}$ is based on the linear model. Its value at the pitch frequency is $\hat{G} = 15.11 + 27.3i$.

Case2. The nonlinearity is included and $\hat{G}$ is based on the nonlinear model. Its value at the pitch frequency is $\hat{G} = 18.03 + 16.13i$.

Again, the use of the nonlinear model results in a better performance and faster convergence for the plunge control compared to the linear model (Figs. 17 to 19).

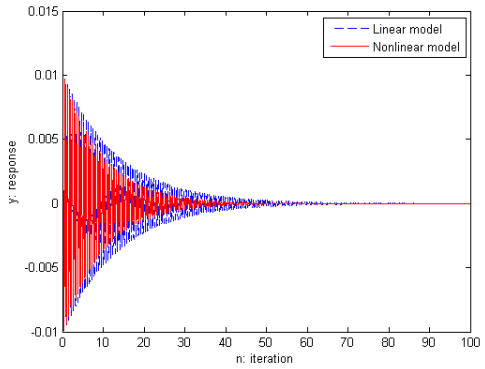

Figure 17. Plunge control: vibration response for the linear (blue dashed line) and nonlinear model (red solid line)

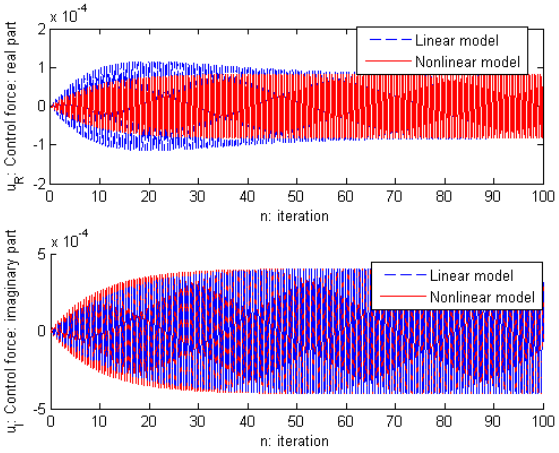

Figure 18. Plunge control force: linear (blue dashed line) and nonlinear model (red solid line)

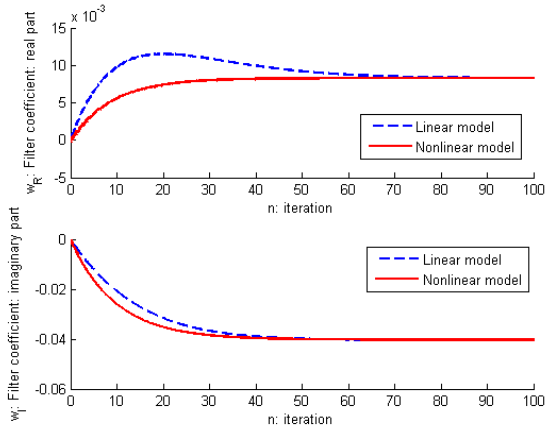

Figure 19. Plunge control: Filter coefficient for the linear (blue dashed line) and nonlinear model (red solid line)

5 CONCLUSIONS

In this paper, a technique based on feedforward control is explored to alleviate the gust response of a nonlinear aeroelastic model. The model is representative of a typical wing section with a trailing-edge flap. The effects of structural nonlinearity, here modeled using a hardening-type spring in the torsional degree of freedom, are first explored in the dynamic response of the open-loop aeroelastic model. As the control strategy requires an approximate model of the plant to be controlled, the effects of structural nonlinearity are then evaluated for the closed-loop response. It is shown that the controller performance is greatly affected by the approximations made in the internal model. To suppress gust-induced vibrations of an intrinsically nonlinear plant, the controller performance is degraded when using a linear representation for the internal plant. Directions for future work include the extension of the current strategy to a multi-input multi-output aeroelastic model and different sources of nonlinearity in the coupled system.

ACKNOWLEDGMENTS

Dr. Maryam Ghandchi Tehrani would like to acknowledge the support provided by EPSRC for her first grant (EP/K005456/1).

REFERENCES

[1] Ghoreyshi, M., Cummings, R.M., Da Ronch, A., and Badcock, K.J. (2013). Transonic Aerodynamic Loads Modeling of X-31 Aircraft Pitching Motions. *AIAA Journal*, 51(10), 2447-2464. doi: 10.2514/1.J052309.

[2] Da Ronch, A., Badcock, K.J., Wang, Y., Wynn, A., and Palacios, R.N. (2012). Nonlinear Model Reduction for Flexible Aircraft Control Design. In *AIAA Atmospheric Flight Mechanics Conference*, AIAA Paper 2012-4404. Minneapolis, MN. doi: 10.2514/6.2012-4404.

[3] Elliott, S. (2001). Signal Processing for Active Control. Academic Press.

[4] Da Ronch, A., Tantaroudas, N. D., Jiffri, S., and Mottershead, J. E. (2014). A Nonlinear Controller for Flutter Suppression: from Simulation to Wind Tunnel Testing. In *AIAA Science and Technology Forum and Exposition*, AIAA-2014-0345. National Harbor, MD. doi: 10.2514/6.2014-0345

[5] Price, S.J., Alighanbari, H., and Lee, B.H.K. (1995). The Aeroelastic Response of a Two-dimensional Airfoil with Bilinear and Cubic Structural Nonlinearities. *Journal of Fluids and Structures*, 9(2), 175-193. doi: 10.1006/jfls.1995.1009

[6] Mottershead, J.E. et al. (2012). Active vibration control experiments on an Agusta-Westland W30 Helicopter Airframe. *IMECHE part C*, 226(6) 1504-1516. doi: 10.1177/0954406211423609

[7] Mottershead, J.E., Ghandchi Tehrani, M., James, S., and Ram, Y.M. (2008). Active Vibration Suppression by pole-placement using measured receptances. Journal of Sound and Vibration, 311(3-5), 1391-1408. doi: 10.1016/j.jsv.2007.10.024